Electronic and elastic properties of non-oxide anti-perovskites from first principles: Superconducting CdCNi$_3$ in comparison with magnetic InCNi$_3$

I. R. Shein[*] and A. L. Ivanovskii

Institute of Solid State Chemistry, Ural Branch of the Russian Academy of Sciences, 620041 Ekaterinburg, Russia
(Received 30 July 2007; revised manuscript received 10 December 2007; published 3 March 2008)

Full-potential linearized augmented plane-wave method with the generalized gradient approximation for the exchange-correlation potential has been applied for the comparative study of structural, elastic, and electronic properties of the synthesized non-oxide anti-perovskites: superconducting CdCNi$_3$ and magnetic InCNi$_3$. The optimized lattice parameters, independent elastic constants (C_{11}, C_{12}, and C_{44}), bulk modules B, compressibility β, shear modules G, and tetragonal shear modules G' are evaluated. The numerical estimates of the elastic parameters of the polycrystalline InCNi$_3$ and CdCNi$_3$ ceramics are performed. The band structures, total and site-projected l-decomposed densities of states, the shapes of the Fermi surfaces, the Sommerfeld coefficients, and the molar Pauli paramagnetic susceptibility for these anti-perovskites are obtained and analyzed in comparison with the available theoretical and experimental data. From our calculations, the stoichiometric CdCNi$_3$ and InCN$_3$ are very much alike in both structural and elastic properties but differ in electronic properties. For InCNi$_3$, the defect-induced magnetism associated with the indium vacancies or Ni atoms substituting for In was found.

PACS number(s): 74.25.Jb, 74.25.Ha, 71.20.Lp

I. INTRODUCTION

Since the discovery of 8 K superconductivity for cubic anti-perovskite MgCNi$_3$,[1] much interest has been paid to other non-oxide anti-perovskites, and the researches of MCNi$_3$ materials, where M are divalent (M^{II}) or trivalent (M^{III}) cations, have been intensively performed. So, the isostructural non-oxide anti-perovskites M^{II}CNi$_3$ and M^{III}CNi$_3$, namely, ZnCNi$_3$,[2] AlCNi$_3$, and GaCNi$_3$,[3–6] have been synthesized and some of their physical properties have been investigated.[5–13]

For the anti-perovskites M^{II}CNi$_3$, the interest is mainly due to the preference of superconductivity over ferromagnetism which is rather unexpected in such Ni-rich compounds. Though the origin of the superconductivity in M^{II}CNi$_3$ is still controversial and remains an open problem, the available data (see Refs. 7 and 8) give some evidences of conventional s-wave BCS-type behavior. The significant achievements in the fundamental understanding of the coupling mechanism and electronic properties of these superconducting M^{II}CNi$_3$ materials were provided by means of the first-principles band-structure calculations.[7–17] It was shown that the density of states (DOS) at the Fermi level, $N(E_F)$, is dominated by Ni d states with admixture of C $2p$ states forming π-type bands. Besides, it has been pointed out[7,8] that the superconducting M^{II}CNi$_3$ compounds tend toward the ferromagnetism due to the existence of a van Hove singularity in the DOS slightly below the Fermi level. As this peak is sharp and the Fermi level lies on the shoulder of the peak, hole doping causes an increase in $N(E_F)$, resulting in a ferromagnetic instability and suppression of the superconducting transition. On the other hand, the electron doping causes a rapid decrease in $N(E_F)$, resulting also in a transition temperature suppression.

This picture has received some confirmations in earlier experiments and calculations.[16,18–24] In this way, the M^{III}CNi$_3$ anti-perovskites can be considered as one-electron

doped M^{II}CNi$_3$ compounds, where the Fermi level is located far from the Ni $3d$ peak, i.e., in the region of a quite low density of states. Thus, it may be expected that M^{III}CNi$_3$ is a Pauli paramagnetic metal.

Really, the anti-perovskites with trivalent metals M^{III} (namely, AlCNi$_3$ and GaCNi$_3$) are nonsuperconducting (see Ref. 13 and references therein), whereas a very surprising fact is the emergence of weak ferromagnetism for these materials reported by Dong *et al.*[5] This circumstance has been discussed by Bannikov *et al.*[12] by means of the density functional theory calculations. The results[13] have shown that AlCNi$_3$ and GaCNi$_3$ are nonmagnetic metals, while their magnetization may be expected at the presence of carbon deficiency.

Very recently, two novel non-oxide anti-perovskites which belong to the group of discussed $M^{II,III}$CNi$_3$ materials, namely, CdCNi$_3$ (Refs. 25 and 26) and InCNi$_3$,[27] have been successfully prepared and some of their physical properties have been investigated.[25–27] According to these results, CdCNi$_3$ is a 3 K superconductor. On the other hand, a quite unusual effect was reported by Tong *et al.*[27] for the indium-containing anti-perovskite: the compound In$_{0.95}$CNi$_3$ behaves as a ferromagnetic metal with a high Curie temperature $T_C \sim 577$ K. It is supposed that the emergence of ferromagnetism may be due to the deviation of the Ni/In ratio from the ideal stoichiometry (Ni/In=3).

In this paper, we report the results of a systematic study by means of the full-potential linearized augmented plane-wave (FLAPW) method within the generalized gradient approximation (GGA) of newly synthesized non-oxide anti-perovskites CdCNi$_3$ and InCNi$_3$ and discuss the trends in their structural, elastic, electronic, and magnetic properties depending on the type of $M^{II,III}$ cations. Our studies have been motivated by the following reasons.

Even though the mentioned experimental results[25–27] for these systems have been published, to our knowledge, no systematic theoretical investigations of the electronic proper-

ties of $CdCNi_3$ and $InCNi_3$ and, in particular, magnetic properties of $InCNi_3$ have been done. Therefore, based on FLAPW-GGA calculations, we calculated the band structures, DOSs, the Fermi surfaces, the Sommerfeld coefficients, and the Pauli paramagnetic susceptibility depending on the type of $M^{II,III}$ cations. It allows us to understand the changes in electronic properties as going from $CdCNi_3$ to $InCNi_3$ in comparison with other anti-perovskites.

Besides, elastic behavior for non-oxide anti-perovskites is of great interest for their potential applications. Therefore, we have predicted the elastic parameters from accurate first-principles FLAPW-GGA calculations not only for $(Cd,In)CNi_3$ monocrystals but also for their polycrystalline states, as these materials are prepared as polycrystalline ceramics. Here, a set of physical parameters of monocrystalline $(Cd,In)CNi_3$ such as optimized lattice parameters, elastic constants (C_{11}, C_{12}, and C_{44}), bulk modules B, compressibility (β), shear modules G, and tetragonal shear modules G' is calculated, and the numerical estimates of elastic modules (B, G), Young's modules (Y), Poisson's ratio (ν), Lamé's coefficients (μ, λ) of the polycrystalline $(Cd,In)CNi_3$ ceramics (in framework of the Voigt-Reuss-Hill approximation) are obtained and analyzed.

Finally, the available experimental and theoretical data have shown that the properties of $(M^{II}, M^{III})CNi_3$ materials are very sensitive to the content of lattice defects—mainly to carbon nonstoichiometry.[28–30] Therefore, on the example of $InCNi_3$, we have investigated the response of the electronic and magnetic behaviors of this material to the presence of various structural defects: (i) vacancies in carbon sublattice, (ii) vacancies in indium sublattice, (iii) vacancies in both In and C sublattices, and (vi) the localization of additional Ni atoms in In sublattice, as it was assumed by Tong *et al.*[27]

II. COMPUTATIONAL METHOD AND MODELS

The considered $(Cd,In)CNi_3$ anti-perovskites adopt[25–27] a cubic structure (e.g., $Pm3m$) consisting of $M^{II,III}$ ions at the corners, carbon at the body center, and Ni at the face centers of the cube. The atomic positions are Ni, $3c$ ($\frac{1}{2}$, $\frac{1}{2}$, 0), $M^{II,III}$, $1a$ (0,0,0), and C, $1b$ ($\frac{1}{2}$, $\frac{1}{2}$, $\frac{1}{2}$). The band-structure calculations were done by means of the full-potential method with mixed basis APW+lo (LAPW) implemented in the WIEN2K suite of programs.[31] The generalized gradient correction (GGA) to the exchange-correlation potential of Perdew *et al.*[32] was used. The electronic configurations were taken to be [Ar] $3d^8 4s^2 4p^0$ for Ni, [Kr] $5s^2 5p^1 4d^{10}$ for In, [Kr] $5s^2 5p^0 4d^{10}$ for Cd, and [He] $2s^2 2p^2$ for carbon. Here, the noble gas cores are distinguished from the subshells of valence electrons. The basis set inside each *muffin-tin* (MT) sphere is split into core and valence subsets. The core states are treated within the spherical part of the potential only and are assumed to have a spherically symmetric charge density confined within MT spheres. The maximum value for partial waves used inside atomic spheres was 12 and the maximum value for partial waves used in the computation of non-muffin-tin matrix elements was 4. The plane-wave expansion with $R_{MT}K_{MAX}$ equal to 8 and k sampling with $10 \times 10 \times 10$ k-point mesh in the Brillouin zone were used. Relativ-

TABLE I. The lattice parameters (a_o, in Å), elastic constants (C_{ij}, in GPa), bulk modulus (B, in GPa), compressibility (β, in GPa^{-1}), shear modulus ($G = C_{44}$, in GPa), and tetragonal shear modulus (G', in GPa) for cubic monocrystalline anti-perovskites $CdCNi_3$ and $InCNi_3$.

Parameters[a]	$CdCNi_3$	$InCNi_3$
a_o	3.8668 (3.844[b])	3.8806 (3.7836[c])
C_{11}	311.46	368.35
C_{12}	126.73	97.02
C_{44} (G)	57.23	43.19
B	188.31	187.46
β	0.00531	0.00533
G'	92.37	135.67

[a]In parentheses—the available experimental data are given.
[b]Reference 26.
[c]Reference 27.

istic effects are taken into account within the scalar-relativistic approximation. The MT radii were 1.79, 2.39, 2.25, and 1.59 a.u. for Ni, Cd, In, and carbon, respectively.

The self-consistent calculations were considered to be converged when the difference in the total energy of the crystal did not exceed 0.01 mRy as calculated at consecutive steps. The DOS was obtained using a modified tetrahedron method.[33]

As a result, the elastic and electronic properties of stoichiometric monocrystalline $CdCNi_3$ and $InCNi_3$ are calculated and then we have utilized the Voigt-Reuss-Hill (VRH) approximation[34] for the estimations of elastic parameters for polycrystalline $(Cd,In)CNi_3$ ceramics. Next, we have focused on the interrelation between the possible structural defects and magnetism of nonstoichiometric anti-perovskite $InCNi_3$. For this purpose, the supercell approach has been employed and, removing the carbon or indium atoms, we simulated the nonstoichiometric materials with formal compositions $InC_{0.875}Ni_3$, $InC_{0.50}Ni_3$, $In_{0.875}CNi_3$, $In_{0.50}CNi_3$, and $In_{0.875}C_{0.875}Ni_3$. Finally, the Ni-rich composition $In_{0.875}Ni_{0.125}CNi_3$ (i.e., $In_{0.875}CNi_{3.125}$) was simulated by replacing Ni→In. Due to the periodic boundary conditions, our calculations were performed for ferromagnetic ordering.

III. RESULTS AND DISCUSSION

A. Lattice constants

First, the equilibrium lattice constants (a_0) for the ideal stoichiometric anti-perovskites $(Cd,In)CNi_3$ were calculated. The results are listed in Table I. As can be seen, $a_0(InCNi_3) > a_0(CdCNi_3)$ and this result can be explained by the atomic radii of $M^{II,III}$: $R(In) = 1.66$ Å $> R(Cd) = 1.56$ Å. It is reasonable to accept that the reduction of the experimentally obtained lattice constant of $InCNi_3$ (Ref. 27) in comparison with $CdCNi_3$ (Ref. 26) occurs from the deviation of the investigated samples[27] from the stoichiometry.

B. Elastic properties

Let us discuss the mechanical parameters for $(Cd,In)CNi_3$ single crystals as obtained within the framework of the

FLAPW-GGA calculations. The values of elastic constants (C_{ij}) for these anti-perovskites are presented in Table I. These three independent elastic constants in a cubic symmetry (C_{11}, C_{12}, and C_{44}) were estimated by calculating the stress tensors on applying strains to an equilibrium structure. All C_{ij} constants for (Cd,In)CNi$_3$ crystals are positive and satisfy the generalized criteria[34–36] for mechanically stable crystals: $(C_{11}-C_{12})>0$, $(C_{11}+2C_{12})>0$, and $C_{44}>0$. Such crystals are characterized by positive values of the bulk modulus $B=(C_{11}+2C_{12})/3$, shear modulus $G=C_{44}$, and tetragonal shear modulus $G'=(C_{11}-C_{12})/2$. The bulk modules of these crystals increase in the sequence $B(\text{InCNi}_3)$ $<B(\text{CdCNi}_3)$, i.e., in reversible sequence to a_0—in agreement with the well-known relationship[37] between B and the lattice constants (cell volume V_o, as $B\sim V_o^{-1}$). This simple trend—when a larger lattice constant leads to a smaller bulk modulus—has been demonstrated also for various perovskitelike materials.[38] Respectively, the compressibility (β $=1/B$) decreases (from InCNi$_3$ to CdCNi$_3$) as the value of a_0 (the size of the M ion) decreases. It was found also for (Cd,In)CNi$_3$: $B>G'>G$; this implies that the parameters limiting the mechanical stability of these materials are the shear modules G.

Note that these elastic parameters are estimated from first-principles FLAPW-GGA calculations of (Cd,In)CNi$_3$ monocrystals. However, these materials have been prepared as polycrystalline ceramics,[25–27] and, therefore, it is useful to evaluate the corresponding parameters for the polycrystalline species. For this purpose we have utilized the VRH approximation (see Refs. 34, 39, and 40). In this approach, the actual effective modulus for polycrystals could be approximated by the arithmetic mean of the two well-known bounds for monocrystals according to Voigt[41] and Reuss.[42] Then, the main mechanical parameters for cubic anti-perovskites, namely, bulk modulus (B), shear modulus (G), Young modulus (Y), Poisson ratio (ν), and Lamé constants (λ,μ) in the two mentioned approximations, Voigt (V)[41] and Reuss (R),[42] are calculated from the elastic constants of single crystals in the following forms.[43]

(a) Bulk modulus,

$$B_{\text{V,R,VRH}}=(C_{11}+2C_{12})/3. \tag{1}$$

(b) Shear modulus,

$$G_{\text{V}}=(C_{11}-C_{12}+3C_{44})/5,$$

$$G_{\text{R}}=5(C_{11}-C_{12})C_{44}/[4C_{44}+3(C_{11}-3C_{12})],$$

$$G_{\text{VRH}}=(G_{\text{V}}+G_{\text{R}})/2. \tag{2}$$

In this way, when a bulk modulus (B_{VRH}) and a shear modulus (G_{VRH}) are obtained from Eqs. (1) and (2), one can calculate the averaged Young modulus (Y_{VRH}) by the expression

$$Y_{\text{VRH}}=9B_{\text{VRH}}/[1+(3B_{\text{VRH}}/G_{\text{VRH}})].$$

Poisson's ratio (ν) and Lamé's coefficients (μ,λ) for the polycrystalline MCNi$_3$ were obtained as

$$\nu=(3B_{\text{VRH}}-2G_{\text{VRH}})/2(3B_{\text{VRH}}+G_{\text{VRH}}),$$

TABLE II. Elastic parameters for polycrystalline CdCNi$_3$ and InCNi$_3$ ceramics as obtained in the Voigt-Reuss-Hill (VRH) approximation.

Parameters		CdCNi$_3$	InCNi$_3$
Bulk modulus (B_{VRH}) (GPa)		188.31	187.46
Shear modulus (G_{VRH}) (GPa)		69.39	69.78
Young's modulus (Y_{VRH}) (GPa)		185.39	185.16
Poisson's ratio (ν)		0.3359	0.3353
Lamé's coefficients	λ	21.87	16.33
(GPa)	μ	71.28	80.18

$$\mu=Y_{\text{VRH}}/2(1+\nu), \quad \lambda=\nu Y_{\text{VRH}}/[(1+\nu)(1-2\nu)].$$

Table II gives the calculated values of the elastic parameters for the polycrystalline (Cd,In)CNi$_3$ species. The bulk modules B_{VRH} slightly decreases as going from CdCNi$_3$ to InCNi$_3$. Since a strong correlation exists between the bulk modulus and hardness of materials,[44] the higher hardness should be for CdCNi$_3$. This conclusion agrees with the behavior of shear modulus G_{VRH}, Table II. Indeed, the hardness of a material is defined as its resistance to another material penetrating its surface, and this resistance is determined by the mobility of dislocations. Thus, one of the determining factors of hardness is the response of interatomic bonds to shear strain.[45] In our case, the shear modulus G_{VRH} is slightly lowered in the sequence CdCNi$_3$ > InCNi$_3$, i.e., a higher bond-restoring energy under elastic shear strain should be for CdCNi$_3$, whereas InCNi$_3$ will remain as a material with the lower hardness. However, the values for B_{VRH} and G_{VRH} of CdCNi$_3$ and InCNi$_3$ are comparable, i.e., the elastic behavior for these polycrystalline materials will differ insignificantly. As shown in Table II, Young modules for these species appear also comparable as well as the Poisson ratio ν.

C. Electronic properties

The band structures and the Fermi surfaces which have been calculated for the equilibrium geometries of (Cd,In)CNi$_3$ are shown in Figs. 1 and 2, respectively. These materials with the same crystal structure have the general features of the band structure. In both compounds, the valence band which extends from −6.3 eV up to the Fermi level E_F=0 eV (for CdCNi$_3$) and from −8.1 up to E_F (for InCNi$_3$) is derived basically from the Ni 3d and C 2p states. The C 2s states are situated in a region from −13 up to −11 eV below the Fermi level and $M^{\text{II,III}}$ (s,p,d) states play a relatively minor role in this interval. For CdCNi$_3$, the occupied Cd 4d bands are localized around −8.5 eV—in the gap between C 2s- and C 2p-like bands; for InCNi$_3$, the occupied In 4d bands are localized around −15.2 eV, i.e., are placed below the C 2s-like bands and are not shown in Figs. 1 and 3.

In the valence region, the C 2p states are partially hybridized with Ni 3d and located below the near-Fermi bands formed mainly from Ni 3d states. From these bands, three are bonding, three are nonbonding, and three are antibonding
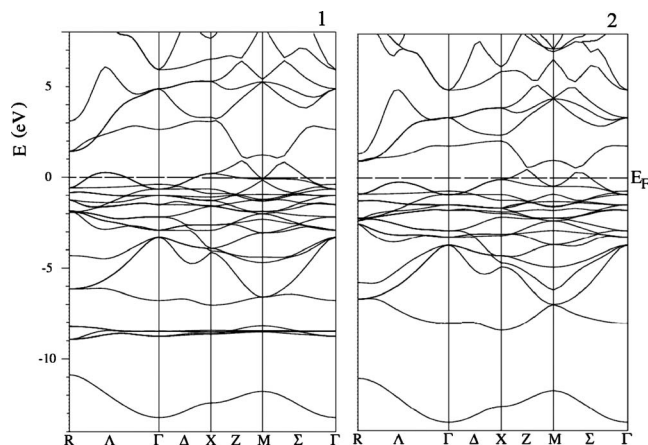
FIG. 1. Band structure of (1) CdCNi$_3$ and (2) InCNi$_3$ along the symmetry lines of the cubic BZ. Fermi level E_F=0 eV.

bands. For CdCNi$_3$, two of antibonding π bands cross E_F. These two bands are confined between −0.7 and 0.9 eV and are half-filled: only two electron states are occupied. The upper band produces the holelike two-sheet Fermi surface centered at the X point and ellipselike along the Γ-R line, Fig. 2. The Fermi surface involves also electronlike sheets around the Γ point and along the R-M line generated by the lower band. This topology of the Fermi surface for CdCNi$_3$ is very similar to the Fermi surfaces of other superconducting M^{II}CNi$_3$ materials.[6,7,16] On the contrary, the Fermi surface changes considerably, Fig. 2, due to the filling of the Ni 3d bands by an additional electron, see Fig. 1.

Let us discuss the main differences of the electronic properties for CdCNi$_3$ and InCNi$_3$ using their densities of states, Fig. 3 and Table III. The overall shape of the total DOS for CdCNi$_3$ is similar to those for InCNi$_3$, except the sharp peak near −9 eV derived from Cd 4d states. Really, the low-lying peaks A are composed from quasicore C 2s states, whereas peaks B and C correspond to partially hybridized C 2p and Ni 3d states, respectively. The most remarkable feature of the DOS for these anti-perovskites is a narrow intense peak D in the vicinity of the Fermi level, Fig. 3. This peak is associated with the quasiflat Ni 3d band aligned along the X-M and M-Γ directions in the Brillouin zone.

For CdCNi$_3$, the Fermi level is located at the high-energy slope of peak D, yielding the high DOS at E_F of $N(E_F)$=4.504 states/eV. The contribution of Ni 3d states to $N(E_F)$ is as much as 72%, and these states are responsible for the
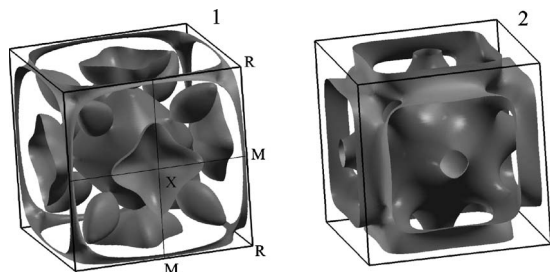

FIG. 2. The Fermi surfaces of (1) CdCNi$_3$ and (2) InCNi$_3$.

metallic properties of material. A small number of C 2p states (at about 7.8%) are mixed with Ni 3d states.

For InCNi$_3$, the increase of the band filling due to the growth of the number of electrons (per cell) leads to the movement of the Fermi level in the region of low binding energies. As a result, E_F in InCNi$_3$ is shifted at 0.5 eV from peak D and lies in the region of relatively small value of DOS. Thus, as expected, $N(E_F)$ for InCNi$_3$ is much less than the value of $N(E_F)$ for CdCNi$_3$, Table III. For InCNi$_3$, the contributions of C 2p and Ni 3d states to $N(E_F)$ are of about 7% and 71%, respectively.

These data allow us to obtain the Sommerfeld constants (γ) and the Pauli paramagnetic susceptibility (χ) for stoichiometric (Cd,In)CNi$_3$ anti-perovskites, assuming the free electron model, as $\gamma=(\pi^2/3)N(E_F)k_B^2$ and $\chi=\mu_B^2N(E_F)$, where $N(E_F)$ is the total DOS at the Fermi level, Table III. It is seen that both γ and χ decrease as going from CdCNi$_3$ to InCNi$_3$—in agreement with the available experimental measurements.[26,27] Our results are also consistent with the Sieberer *et al.* data.[13] They estimated Sommerfeld constants γ and the Pauli paramagnetic susceptibility χ for M^{II}CNi$_3$ and M^{III}CNi$_3$ as γ=9.8–10.8 mJ/(mol K^2) (M^{II}=Mg,Zn) and 4.9–4.3 mJ/(mol K^2) (M^{III}=Al,Ga) and χ=(1.34–1.48)×10^{-4} emu/mol (M^{II}=Mg,Zn) and (0.67–0.59)×10^{-4} emu/mol (M^{III}=Al,Ga).

Additionally, the calculated Sommerfeld constant γ^{theor} may be useful for simple estimations[46] of the average electron-phonon coupling constant λ (for superconducting CdCNi$_3$) as $\gamma^{exp}=\gamma^{theor}(1+\lambda)$. Within a very crude estimate, using our γ^{theor} for CdCNi$_3$ and the measured[26] γ^{exp} [~18 mJ/(mol K^2)], we obtain an empirical value of λ of about 0.7, i.e., CdCNi$_3$ is within the weak coupling limit. For comparison, for other superconducting M^{II}CNi$_3$ anti-perovskites, the available experimental and theoretical (including the lattice dynamic effects and the phonon DOS calculations) estimations of λ vary from 1.4 to 0.66.[8]

D. Role of lattice defects and substitutions in magnetization of InCNi$_3$

As reported in Ref. 27, InCNi$_3$ behaves as a ferromagnetic metal—in contradiction to the results[13] which show that related anti-perovskites AlCNi$_3$ and GaCNi$_3$ are nonmagnetic metals. In order to figure out the possible factors for magnetism of InCNi$_3$, we first discuss qualitatively the magnetic behavior of stoichiometric (Cd,In)CNi$_3$, using Stoner's criterion[47] $N(E_F)I>1$, where I is the exchange-correlation integral. Accepting Janak's[47] value I=0.5 eV (for Ni) and using our calculated values for paramagnetic DOS at E_F, i.e., for CdCNi$_3$, $N^{Ni}(E_F)$=1.131 states/eV atom, and for InCNi$_3$, $N^{Ni}(E_F)$=0.646 states/eV atom, we have estimated Stoner's factor $S=N(E_F)I$ for these materials at about 0.57 and 0.32, respectively. Note that the available estimations of Stoner's exchange enhancement parameter S for the related nonmagnetic $M^{II,III}$CNi$_3$ materials are comparable to these results (0.64 for MgCNi$_3$,[15] 0.65 for ZrCNi$_3$,[10] and 0.24 and 0.21 for AlCNi$_3$ and GaCNi$_3$ according to the FLAPW-GGA calculations[13]). So, the stoichiometric (Cd,In)CNi$_3$ anti-
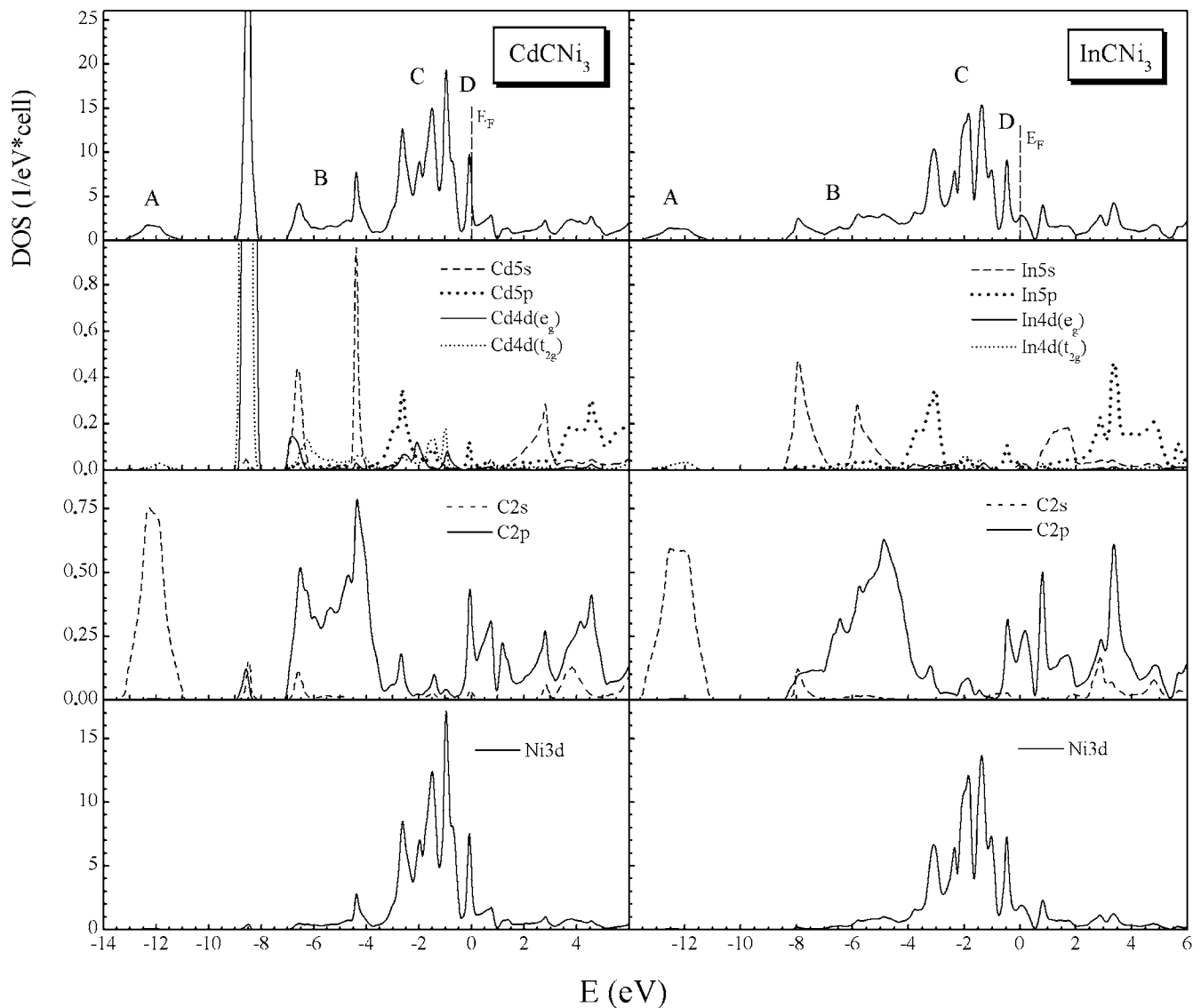
FIG. 3. Density of states (DOS) for (1) $CdCNi_3$ and (2) $InCNi_3$. The results for the total (top) and atomic resolved l-decomposed (bottom) DOSs are shown.

perovskites do not satisfy the Stoner criterion and thus they are paramagnetic. On the other hand, $CdCNi_3$ is closer to a ferromagnetic instability than $InCNi_3$, for which the ferromagnetism was reported.[27]

To explain this unexpected situation, we have examined the role of possible structural defects in $InCNi_3$. For this purpose, the magnetic behavior of $InCNi_3$ with various amounts of carbon, indium, both carbon and indium vacancies, as well as with a substitutional $Ni^{(s)}$ defect on In site was considered, see Table IV. The results of our calculations indicate that the presence of carbon vacancies (up to 50%) retain the nonmagnetic state of the system. On the other hand, the magnetism in $InCNi_3$ may be induced by 50% In vacancies, Fig. 4. For this system (with nominal composition $In_{0.50}CNi_3$), the energy preference of ferromagnetic state versus paramagnetic is at about 0.12 eV.

Apparently, the additional Ni atoms may be responsible for the enhancement of metallicity of this material and for this proximity to magnetism. Thus, our calculation was performed for $Ni^{(s)}$ atom substituting the indium position. This means the nonstoichiometric compound (i.e., $Ni/In > 3$) with nominal composition $In_{0.875}CNi_{3.125}$. This additional $Ni^{(s)}$ placed in $1a$ (0,0,0) position forms a cluster with the rest of the Ni atoms located in $3c$ $(\frac{1}{2},\frac{1}{2},0)$ positions. We have found that $In_{0.875}CNi_{3.125}$ also acquires magnetization.

Thus, these results show that, in principle, two types of lattice defects (indium vacancies and substitutional $Ni^{(s)}$ atoms) may be responsible for the magnetic behavior of nonstoichiometric In-Ni-C species. What from these defects is more preferable? For the answer, we have estimated the relative stability of these two nonstoichiometric In-Ni-C species: $In_{0.5}CNi_3$ versus $In_{0.875}CNi_{3.125}$ in comparison with stoichiometric $In_{0.5}CNi_3$. For this purpose, their Gibbs free energies $(G = \Delta H + PV - TS)$ should be obtained. Since our calculations are performed at zero temperature and zero pressure, G becomes equal to the enthalpy of formation ΔH, which can be estimated from the total energies of In-C-Ni compounds and its constituents. Here, the reactions of phase formation

TABLE III. Total and site-projected l–decomposed densities of states at the Fermi level [$N(E_F)$, in states/eV cell], Sommerfeld coefficients [γ, in mJ/(mol K^2)], and molar Pauli paramagnetic susceptibility (χ, in 10^{-4} emu/mol) for cubic anti-perovskites CdCNi$_3$ and InCNi$_3$.

Parameters[a]	CdCNi$_3$	InCNi$_3$
$N(E_F)$(C 2s)	0.018	0.003
$N(E_F)$(C 2p)	0.331	0.207
$N(E_F)$(Ni 4s)	0.057	0.033
$N(E_F)$(Ni 4p)	0.078	0.056
$N(E_F)$(Ni 4d)	3.258	1.848
$N(E_F)$(Ni)	3.393	1.937
$N(E_F)$(M s)	0.001	0.029
$N(E_F)$(M p)	0.030	0.040
$N(E_F)$(M d)	0.013	0.008
$N(E_F)$ (total)	4.504	2.707
γ	10.62 (18[b])	6.38 (14.1[c])
χ	1.46	0.88

[a]In parentheses—the available experimental data are given.
[b]Reference 26.
[c]Reference 27.

from the simple substances are usually used for the estimation of ΔH. In our case, the formation energies (E_f) of In$_{1-x}$CNi$_{3+y}$ phases with respect to the metallic Ni, indium, and graphite (C^g) in the formal reaction In$_{1-x}$CNi$_{3+y}$ $\leftrightarrow$ $(1-x)$In+$(3+y)$Ni+C^g are defined as E_f(In$_{1-x}$CNi$_{3+y}$) $=E_{tot}$(In$_{1-x}$CNi$_{3+y}$)$-[(3+y)E_{tot}$(Ni)$+(1-x)E_{tot}$(In)$+E_{tot}$(C^g)]. In this way, we have obtained the formation energies (E_f) of stoichiometric InCNi$_3$ and nonstoichiometric In$_{0.5}$CNi$_3$ and In$_{0.875}$CNi$_{3.125}$: -2.09, $+2.80$, and -0.71 eV per cell. Thus, negative values of E_f point out the formation of stable phases, and it should be concluded that the formation of the Ni-rich phase In$_{0.875}$CNi$_{3.125}$ is favorable—as compared with In-deficient species which are unstable.

Going back to the magnetization of In$_{0.875}$CNi$_{3.125}$, we shall note that our calculated value for paramagnetic DOS at E_F for the additional Ni$^{(s)}$ (1.744 states/eV atom Ni$^{(s)}$) is much higher than the corresponding value for stoichiometric InCNi$_3$ (0.646 states/eV atom Ni), leading to the increase of Stoner's exchange enhancement parameter and magnetic in-

TABLE IV. Magnetic moments (in μ_B) for InCNi$_3$ with defects.

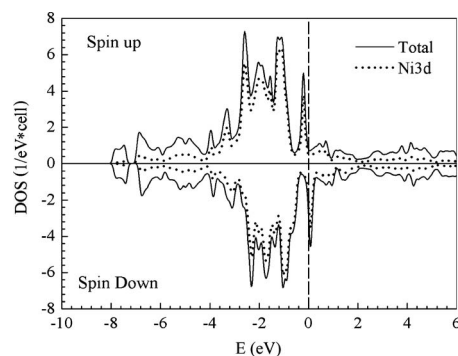| System	MM (Ni)	MM (total)
In$_{0.875}$CNi$_3$	0	0
InC$_{0.875}$Ni$_3$	0	0
In$_{0.875}$C$_{0.875}$Ni$_3$	0	0
InC$_{0.50}$Ni$_3$	0	0
In$_{0.50}$CNi$_3$	0.253[a]	0.842[b]
In$_{0.875}$CNi$_{3.125}$	0.373[a]	0.033[b]

[a]Per single Ni$^{(s)}$ atom.
[b]Per f.u.

FIG. 4. Density of states (DOS) for nonstoichiometric In$_{0.50}$CNi$_3$. The total (full lines) and Ni d resolved (dotted lines) DOSs are shown.

stability of In$_{0.875}$CNi$_{3.125}$. We have found that the energy difference between the stable ferromagnetic and paramagnetic states is at about 0.02 eV.

Finally, in In$_{0.875}$CNi$_{3.125}$, the additional Ni$^{(s)}$ has no nearest carbon neighbors; the Ni-C hybridization is absent. This leads to the exchange splitting of Ni$^{(s)}$ $3d^{\uparrow\downarrow}$ orbitals, as depicted in Fig. 5. So, by the substitution of indium by nickel, a magnetization essentially localized on Ni$^{(s)}$ (0.373 μ_B) arises, whereas the other atoms surrounding the Ni$^{(s)}$ have a very small negative induced magnetic moment (at about -0.008 μ_B) due to the overlapping with spin-polarized Ni$^{(s)}$ states. Thus, the magnetic polarization in In$_{0.875}$CNi$_{3.125}$ seems to be quite the local effect, without affecting atoms away from the substitutional atom.

IV. CONCLUSIONS

In conclusion, we have performed first principles FLAPW-GGA calculations for comparative study of the structural, elastic, and electronic properties of the synthe-
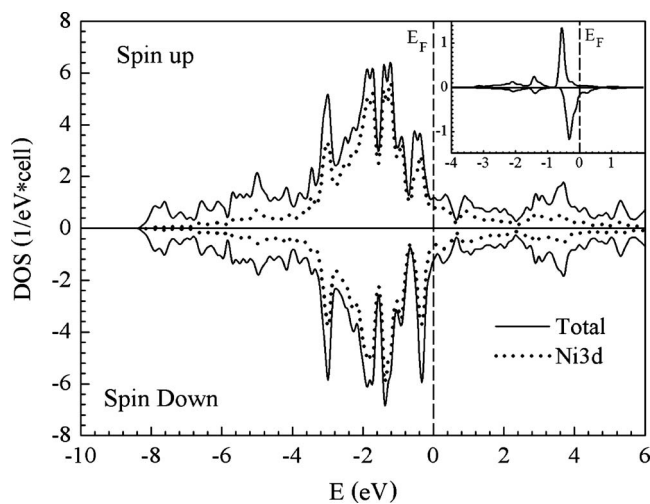

FIG. 5. Density of states (DOS) for In$_{0.875}$CNi$_{3.125}$. The total (full lines) and Ni d resolved (dotted lines) DOSs are shown. Inset: DOS for Ni$^{(s)}$ atom substituting indium.

sized non-oxide anti-perovskites: superconducting $CdCNi_3$ and magnetic $InCNi_3$. From our calculations, the stoichiometric $CdCNi_3$ and $InCN_3$ are very similar in both structural and elastic properties. It was found for both anti-perovskites that $B > G' > G$, i.e., the parameters limiting the mechanical stability of these materials are the shear modules G. Also, our numerical estimations for $(Cd,In)CNi_3$ ceramics (in the framework of the Voigt-Reuss-Hill approximation) show that the elastic behavior for these polycrystalline materials should differ insignificantly.

On the other hand, our calculations clearly show that stoichiometric $CdCNi_3$ and $InCNi_3$ are nonmagnetic metals and are far away from a magnetic ground state. To find the tendencies toward magnetism, the separate calculations were carried out for the possible scenarios of magnetization of $InCNi_3$ induced by indium, carbon vacancies or due to a substitutional $Ni^{(s)}$ on the In site. Both In vacancies and substitutional $Ni^{(s)}$ in $InCNi_3$ were found to lead to spin-polarized ground states. However, while substitution of In for $Ni^{(s)}$ is more energetically preferable and results in the spin polarization of $Ni^{(s)}$ atom (i.e., creates a local magnetism), the presence of In vacancies leads to a magnetization of all atoms in the Ni sublattice.

*Corresponding author; shein@ihim.uran.ru

[1] T. He, Q. Huang, A. P. Ramirez, Y. Wang, K. A. Regan, N. Rogado, M. A. Hayward, M. K. Haas, J. S. Slusky, K. Inumaru, H. W. Zandbergen, N. P. Ong, and R. J. Cava, Nature (London) **411**, 54 (2001).

[2] M. S. Park, J. S. Giim, S. H. Park, Y. W. Lee, S. I. Lee, and E. J. Choi, Supercond. Sci. Technol. **17**, 274 (2004).

[3] J. B. Goodenough and M. Longo, in *Magnetic and Other Properties of Oxides and Related Compounds*, edited by K.-H. Hellwege and A. M. Hellwege, Landolt-Börnstein, Group III, New Series, Vol. 4, Pt. A (Springer-Verlag, Berlin, 1970), pp. 266–269.

[4] R. E. Schaak, M. Avdeev, W.-L. Lee, G. Lawes, H. W. Zandbergen, J. D. Jorgensen, N. P. Ong, A. P. Ramirez, and R. J. Cava, J. Solid State Chem. **177**, 1244 (2004).

[5] A. F. Dong, G. C. Che, W. W. Huang, S. L. Jia, H. Chen, and Z. X. Zhao, Physica C **422**, 65 (2005).

[6] P. Tong, Y. P. Sun, X. B. Zhu, and W. H. Song, Phys. Rev. B **73**, 245106 (2006).

[7] A. L. Ivanovskii, Phys. Solid State **45**, 1829 (2003).

[8] S. Mollah, J. Phys.: Condens. Matter **16**, R1237 (2004).

[9] M. D. Johannes and W. E. Pickett, Phys. Rev. B **70**, 060507(R) (2004).

[10] I. R. Shein, K. I. Shein, and A. L. Ivanovskii, Metallofiz. Noveishie Tekhnol. **26**, 1193 (2004).

[11] C. M. I. Okoye, Solid State Commun. **136**, 605 (2005).

[12] V. V. Bannikov, I. R. Shein, and A. L. Ivanovskii, Phys. Solid State **49**, 1626 (2007).

[13] M. Sieberer, P. Mohn, and J. Redinger, Phys. Rev. B **75**, 024431 (2007).

[14] S. B. Dugdale and T. Jarlborg, Phys. Rev. B **64**, 100508(R) (2001).

[15] J. H. Shim, S. K. Kwon, and B. I. Min, Phys. Rev. B **64**, 180510(R) (2001).

[16] D. J. Singh and I. I. Mazin, Phys. Rev. B **64**, 140507(R) (2001).

[17] I. G. Kim, J. I. Lee, and A. J. Freeman, Phys. Rev. B **65**, 064525 (2002).

[18] H. Rosner, R. Weht, M. D. Johannes, W. E. Pickett, and E. Tosatti, Phys. Rev. Lett. **88**, 027001 (2001).

[19] T. G. Kumary, J. Janaki, A. Mani, S. M. Jaya, V. S. Sastry, Y. Hariharan, T. S. Radhakrishnan and M. C. Valsakumar, Phys. Rev. B **66**, 064510 (2002).

[20] A. Das and R. K. Kremer, Phys. Rev. B **68**, 064503 (2003).

[21] T. Klimczuk, V. Gupta, G. Lawes, A. P. Ramirez, and R. J. Cava, Phys. Rev. B **70**, 094511 (2004).

[22] S.-H. Park, Y. W. Lee, J. Giim, S.-H. Jung, H. C. Ri, and E. J. Choi, Physica C **400**, 160 (2004).

[23] T. Klimczuk, M. Avdeev, J. D. Jorgensen, and R. J. Cava, Phys. Rev. B **71**, 184512 (2005).

[24] I. R. Shein, A. L. Ivanovskii, E. Z. Kurmaev, A. Moewes, S. Chiuzbian, L. D. Finkelstein, M. Neumann, Z. A. Ren, and G. C. Che, Phys. Rev. B **66**, 024520 (2002).

[25] M. Uehara, T. Amano, S. Takano, T. Kori, T. Yamazaki, and Y. Kimishima, Physica C **440**, 6 (2006).

[26] M. Uehara, T. Yamazaki, T. Kori, T. Kashida, Y. Kimishima, and I. Hase, J. Phys. Soc. Jpn. **76**, 034714 (2007).

[27] P. Tong, Y. P. Sun, X. B. Zhu, and W. H. Song, Solid State Commun. **141**, 336 (2007).

[28] L. Shan, K. Xia, Z. Y. Liu, H. H. Wen, Z. A. Ren, G. C. Che, and Z. X. Zhao, Phys. Rev. B **68**, 024523 (2003).

[29] H. D. Yang, S. Mollah, W. L. Huang, P. L. Ho, H. L. Huang, C.-J. Liu, J.-Y. Lin, Y.-L. Zhang, R.-C. Yu, and C.-Q. Jin, Phys. Rev. B **68**, 092507 (2003).

[30] P. J. T. Joseph and P. P. Singh, J. Phys.: Condens. Matter **18**, 5333 (2006).

[31] P. Blaha, K. Schwarz, G. K. H. Madsen, D. Kvasnicka, and J. Luitz, WIEN2K, An augmented plane wave plus local orbitals program for calculating crystal properties, Vienna University of Technology, Vienna, 2001.

[32] J. P. Perdew, K. Burke, and M. Ernzerhof, Phys. Rev. Lett. **77**, 3865 (1996).

[33] P. E. Blöchl, O. Jepsen, and O. K. Andersen, Phys. Rev. B **49**, 16223 (1994).

[34] G. Grimvall, *Thermophysical Properties of Materials* (North-Holland, Amsterdam, 1986).

[35] J. Wang, S. Yip, S. R. Phillpot, and D. Wolf, Phys. Rev. Lett. **71**, 4182 (1993).

[36] S. Yip, J. Li, M. Tang, and J. Wang, Mater. Sci. Eng., A **317**, 236 (2001).

[37] M. L. Cohen, Phys. Rev. B **32**, 7988 (1985).

[38] R. D. King-Smith and D. Vanderbilt, Phys. Rev. B **49**, 5828 (1994).

[39] R. Hill, Proc. Phys. Soc., London, Sect. A **65**, 349 (1952).

[40] D. H. Chung, Philos. Mag. **8**, 833 (1963).

[41] W. Voigt, *Lehrbuch der Kristallphysik* (Teubner, Leipzig, 1928).

[42] A. Reuss, Z. Angew. Math. Mech. **9**, 49 (1929).

[43] E. Schreiber, O. L. Anderson, and N. Soga, *Elastic Constants and Their Measurements* (McGraw-Hill, New York, 1973).

[44] J. Haines, J. M. Leger, and G. Bocquillon, Annu. Rev. Mater. Res. **31**, 1 (2001).

[45] S.-H. Jhi, J. Ihm, S. G. Louie, and M. L. Cohen, Nature (London) **399**, 132 (1999).

[46] Ch. Walti, E. Felder, C. Degen, G. Wigger, R. Monnier, B. Delley, and H. R. Ott, Phys. Rev. B **64**, 172515 (2001).

[47] J. F. Janak, Phys. Rev. B **16**, 255 (1977).